International Journal of Rock Mechanics & Mining Sciences 53 (2012) 101–110

Contents lists available at SciVerse ScienceDirect

International Journal of Rock Mechanics & Mining Sciences

journal homepage: www.elsevier.com/locate/ijrmms

Technical Note

Case study on microseismic effect of coal and gas outburst process

Cai-Ping Lu [a,b,c,*], Lin-Ming Dou [a,b], Hui Liu [a], Hai-Shun Liu [d], Biao Liu [a], Bin-Bin Du [a]

[a] School of Mining Engineering, China University of Mining and Technology, Xuzhou, Jiangsu 221116, PR China
[b] State Key Laboratory of Coal Resources and Mine Safety, China University of Mining and Technology, Xuzhou, Jiangsu 221116, PR China
[c] State Key Laboratory of Deep Coal Mining and Environment Protection, Huainan Mining Industry Group, Huainan, Anhui 232001, PR China
[d] School of Science, China University of Mining and Technology, Xuzhou, Jiangsu 221116, PR China

ARTICLE INFO

Article history:
Received 13 August 2011
Received in revised form
20 February 2012
Accepted 3 May 2012
Available online 24 May 2012

1. Introduction

Since the first reported coal and gas outburst occurred in the Issac Colliery, Loire coal field, France, in 1843 [1], this hazard has occurred in most coal-producing countries and has posed a challenge to coal mine safety production [2–4]. Lama and Bodziony [1] reported that over 30,000 outbursts have occurred worldwide, but their total included only about 10,000 in China. More recent reports showed more than 14,000 outbursts have occurred in China [5].

Many researchers have studied relationships between coal outbursts and geological factors, such as coal seam thickness, coal rank, coal seam age, current burial depth, and distance to plutons, with different conclusions for different coal fields and regions because of the complexity of the causative mechanisms. Coal and gas outburst is an engineering geological hazard by mining, and in Australia, Canada, China, Europe, Japan, the United States, and Russia, this hazard often happened. Besides, gas combustion and explosion was sometimes caused indirectly by coal and gas outburst, which would cause substantial damage to property and casualties. Coal and gas outburst, gas and dust explosion induced is still the first harm to safety production, its prediction and prevention work is global issue.

Coal and gas outburst essentially is a conversion process between function and energy, which converts the potential accumulated energy of the source into the kinetic energy. Outburst process generally can be divided into two stages: stimulation and occurrence, which sometimes can be distinguished obviously, however, it is very difficult to distinguish these two stages because the transient stimulation process depends on coal and rock load state and stress level of outburst source [6]. Dynamic stress of coal and rock material closest to outburst source will be imposed by the additional impact load produced by blasting in mining process, especially shock wave induced by roof strata fracture, which will stimulate the sudden rupture of coal material in the critical stress condition, produce the fissures of outburst channel, and also accelerate the escape velocity of gas. As a final result, coal and gas outburst will easily be induced by converting potential energy into kinetic energy in very short time surrounding source materials [7]. Accumulated gas was extruded by shock wave of roof fracture, escaped from coal breakage, and mixed with air in roadway. Finally, the explosive mixture air was formed. If encountered with fire, the gas explosion will happen [8].

From retrieving related-literature, it is found that many studies have been conducted on the mechanism and prediction methods of coal and gas outburst. For example, Zhou [9] put forward the rheology hypothesis of coal and gas outburst, by which the mechanism of outburst could be better clarified. On this basis, He et al. [10–12] established the electromagnetic emission (EME) abnormal discriminant model and criterion based on the EME rules of coal and gas outburst process, and the method had been applied to predict outburst in some outburst dangerous coal mines. Zhang [13] developed a visual system of coal and gas outburst regional prediction based on geographic information system (GIS), which had been applied to zone the dangerous region in Panyi coal mine of Huainan mining industry group (HNMIG). Tang [14] believed that micro-fissure fracture is the common precursory characteristic of coal and rock dynamic hazard by mining such as rockburst, water inrush, and coal and gas outburst, and proposed to predict outburst using microseism (MS) technology by introducing Canadian ESG MS monitoring system in Xinzhuangzhi coal mine of HNMIG. Jiang [15] tried to predict coal and gas outburst by high-precision MS monitoring

* Corresponding author at: School of Mining Engineering, China University of Mining and Technology, Xuzhou, Jiangsu 221116, PR China.
Tel./fax: +86 516 83885904.
E-mail address: cplucumt@126.com (C.-P. Lu).

1365-1609/$ - see front matter
http://dx.doi.org/10.1016/j.ijrmms.2012.05.009

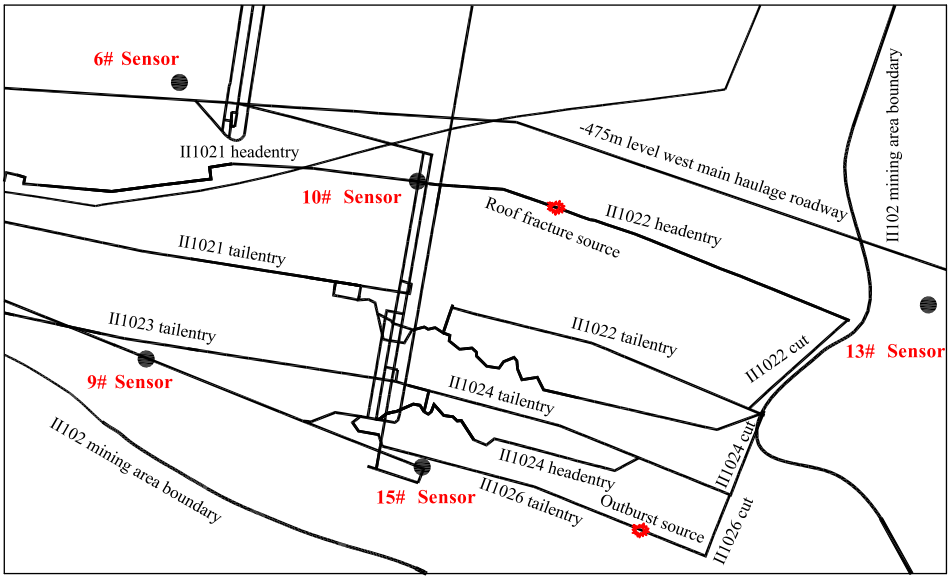

Fig. 1. Optimization arrangement of MS stations in II102 mining area.

technology on basis of gas occurrence, geology and mining factors, etc. Mckavanagh [16] firstly recorded the micro-acoustic emission (MAE) signals of coal and gas outburst in West Cliff coal mine in 1980, and found that the signal frequency is 100–5 kHz. Leighton [17] found several rapid micro-fracture phenomena before coal and gas outburst by MS monitoring system in 1984. Davies [18] revealed that MAE and MS signals of roof strata fracture could be recorded before coal and gas outburst. Peter [19] found that MS signal frequency-spectrum monitored showed "O" type distribution before a typical of coal and gas outburst and the central frequency was about 32 Hz, simultaneously proposed a method to prevent coal and gas outburst by harmonic vibration for controlling gas releasing velocity. Stephen [20] studied the relationship between permeability and MAE signal characteristic parameters for samples of the outburst-prone sandstone of triaxial pressures and axial stresses up to failure, and experimental data suggested that microcracking in the sandstone prior to compressive failure could not significantly enhance permeability but there may be local pockets of higher permeability within the sandstone. Cao [5] found that coal and gas outbursts associated with reverse faults can be expected to occur more frequently, and proposed to carry out stress measurements in the two walls of reverse faults in order to investigate any relationship to outburst occurrence. María [21] designed a kind of gas-measurement-tube set to determine outburst prone areas, and applied it in Riosa-Olloniego coalfield, Spain, and subsequently proposed a method to prevent outburst by enhancing permeability using high pressure water infusion and the exploitation of a protective coal seam. Talebi [22] reported that cases of outburst were described as a result of the ejection of finely pulverized sandstone into the openings. An "intrinsically safe" portable MS monitoring system, designed for the Sydney coal field, was installed in Phalen Colliery at a depth of 695 m.

As a consequence of the above, the evaluation of coal and gas outburst danger using MS and other technologies has been researched by extensive experiments in detail, especially, the MAE monitoring of outbursts on the basis of coal and rock fracture also has been discussed fruitfully. However, the frequency-spectrum evolution rules of MS signals before and during outburst, especially the MS precursory effect of outburst is still lack of field experimental research.

Table 1
The three-dimensional coordinates of 5 sensors.

Sensor number	*x* (m)	*y* (m)	*z* (m)
6#	39463296.42	3727226.44	−475.00
9#	39465389.09	3727996.08	27.40
10#	39462915.51	3727443.76	−576.65
13#	39462024.29	3727733.79	−461.70
15#	39462934.25	3727967.76	−693.83

Table 2
Gas basic parameters measured results.

Position	Coal seam	Gas pressure (MPa)	Adsorption constant		Elevation (m)
			a	*b*	
II102 mining area					
West main roadway	10#	2	17.33	1.0556	−727
Ventilation dip roadway	10#	0.55	18.454	1.067	−668
Ventilation dip roadway	10#	0.5	–	–	−660

With the guidance of SOS broadband MS monitoring system developed by the Polish Mining Research Institute, based on a typical of coal and gas outburst hazard that happened in II1026 driving working face of Haizi coal mine belonged to Huaibei mining industry group, the outburst process was recorded clearly and completely, and analyzed in detail to reveal the mechanism and MS effect of outburst.

2. MS monitoring and analysis of coal and gas outburst

2.1. Introduction of MS monitoring system

SOS MS monitoring system mainly includes the recorder, analyzer, sensors, and digital transmission system, etc., which commonly has

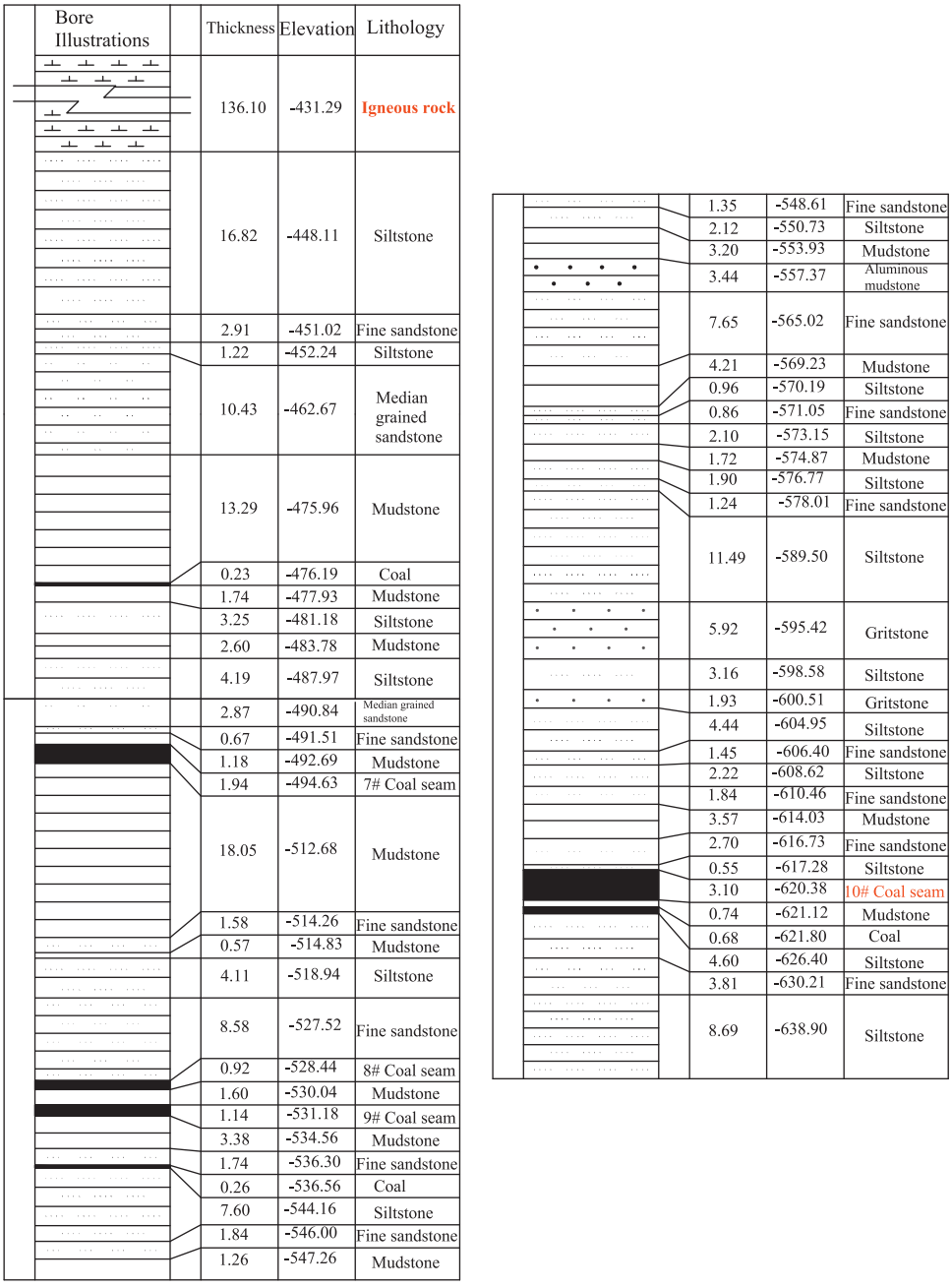

Fig. 2. Column illustration of 21B3 geological borehole in II102 mining area.

Table 3
9 MS events recorded and marked clearly.

Event label	Time	*X* coordinate (m)	*Y* coordinate (m)	*Z* coordinate (m)	Energy (J)	Position
a	1:47:15	39462779	3727716	−512.75	350	Roof of II1024 gob
b	1:47:21	39462530	3728204	−759.15	8414	Near II1026 head-on
c	1:47:23	39462522	3728136	−742.16	5475	Near II1026 head-on
d	1:47:27	39462503	3728195	−754.63	7966	Near II1026 head-on
e	1:47:28	39462484	3728207	−782.91	2574	Near II1026 head-on
f	1:47:31	39462519	3728127	−788.64	2425	Near II1026 head-on
g	1:47:33	39462508	3728173	−751.53	2077	Near II1026 head-on
h	1:47:47	39462485	3728210	−770.86	1805	Near II1026 head-on
i	1:48:07	39462497	3728141	−677.19	8547	II1026 tailentry head-on

16 input channels, the sampling rate is 500 Hz, A/D converter is 16 bits, and the maximum data transmission rate is 1 MB/s. SOS MS system can immediately, continuously, and automatically collect and filter shock signal, and accurately calculate the occurrence time, energy, and space three-dimensional coordinates of shock event ($E > 100$ J) using Powell location algorithm, and the

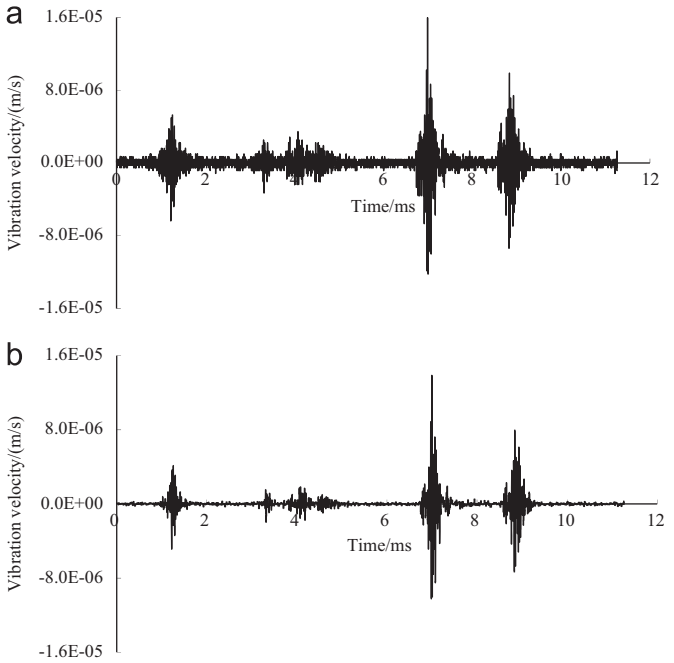

Fig. 3. Waveform change before and after the noise removal (1:47:15-10#). (a) Vibration-time curve of waveform before the noise removal. (b) Vibration-time curve of waveform after the noise removal.

constant velocity model is proposed for location, which is calibrated by time residual error of arrival of a number of large shock signals. The broadband sensor is designed to moving-coil type speed sensor, the resonance frequency is 4.5 ± 0.75 Hz and its frequency band width is 1–600 Hz, the response of which is flattened by filter and cable noise can be eliminated through 50 Hz band-pass filter of the controllable switch. The horizontal positioning error of the system is less than 20 m, and the vertical error is less than 30 m, if the sensors optimization arrangement can be made.

SOS MS system of Haizi coal mine was installed and operated in early December 2008. A three-dimensional monitoring pattern consisted of 16 MS stations, arranged and installed in the underground roadway and the surface bedrock borehole. Based on present mining activity and the igneous rock structure flexural deformation caused in II102 mining area, 5 sensors (6#, 9#, 10#, 13# and 15#) of MS system mainly covered and monitored the igneous rock influencing scope of II102 mining area (As shown in Fig. 1). Table 1 shows the three-dimensional coordinates of the above-mentioned 5 sensors, and 9# sensor was located at surface (Surface vertical elevation is 26.5–28.6 m).

2.2. Production and geological condition of II102 mining area

II102 mining area overall is a monoclinic structure, and the vertical elevation is from -475 to -700 m. The main mining seam is #10 coal seam belonged to the non-outburst prone coal

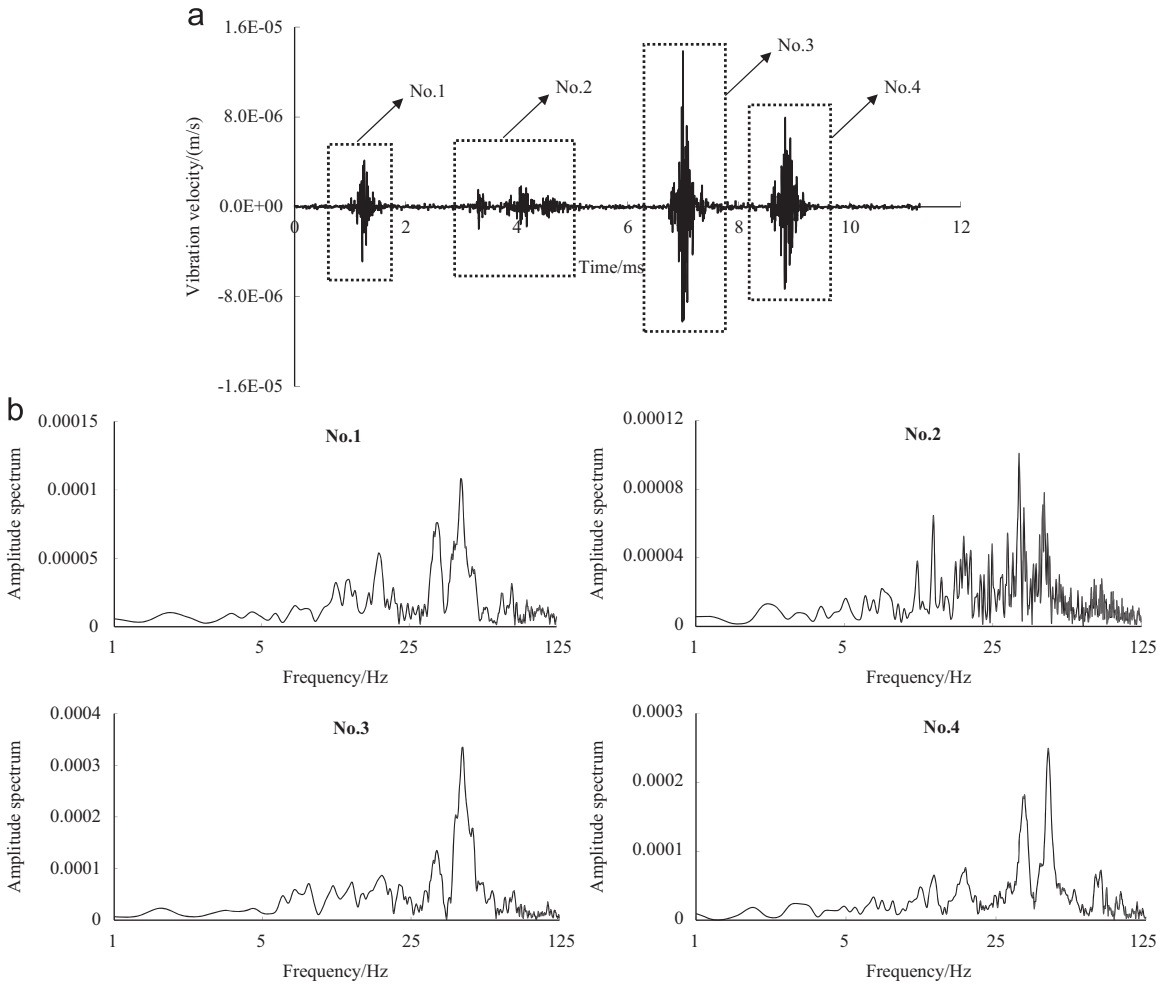

Fig. 4. Curves of vibration velocity-time and amplitude spectrum-frequency (1:47:15-10#). (a) Vibration velocity-time. (b) Amplitude spectrum-frequency.

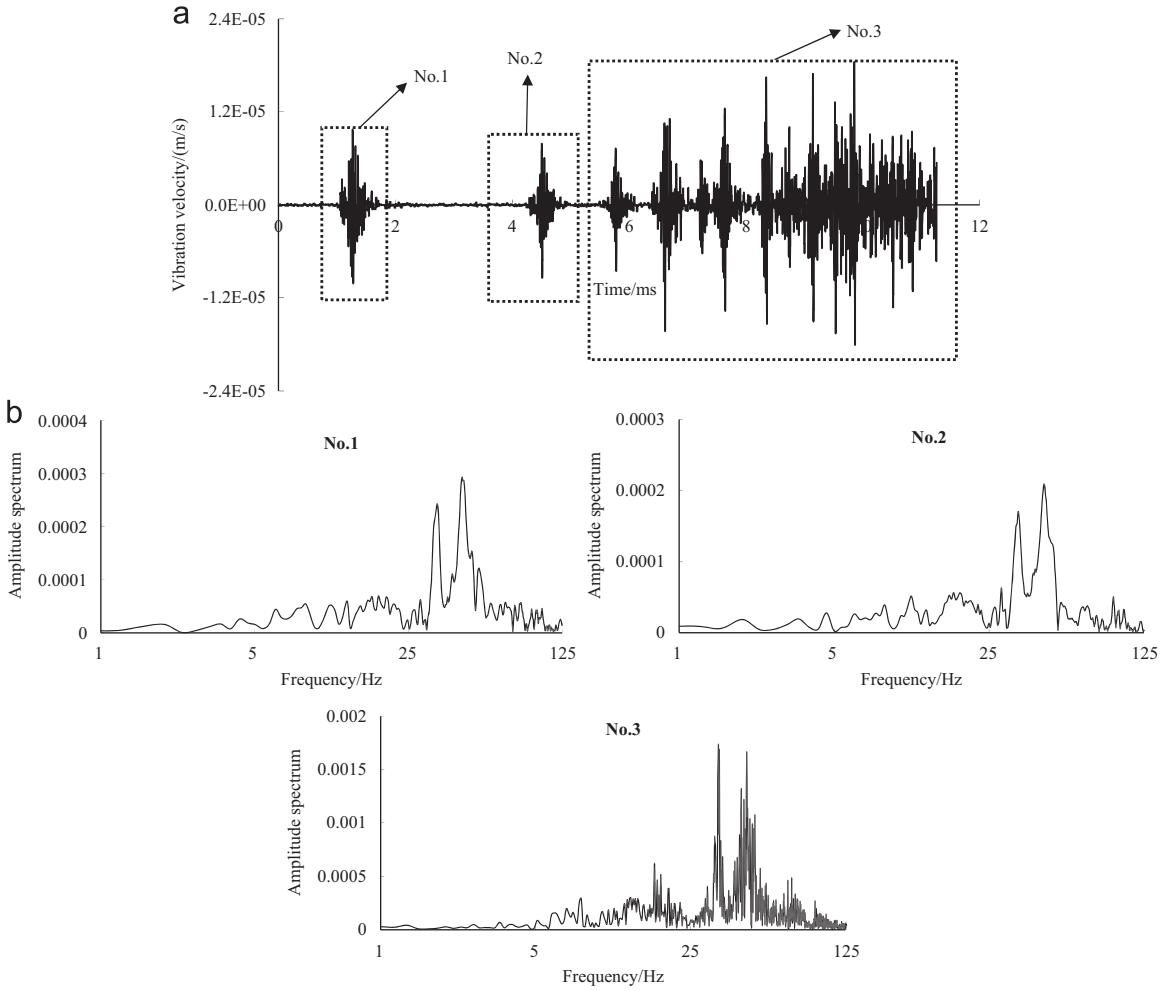

Fig. 5. Curves of vibration velocity-time and amplitude spectrum-frequency (1:47:27-10#). (a) Vibration velocity-time. (b) Amplitude spectrum-frequency.

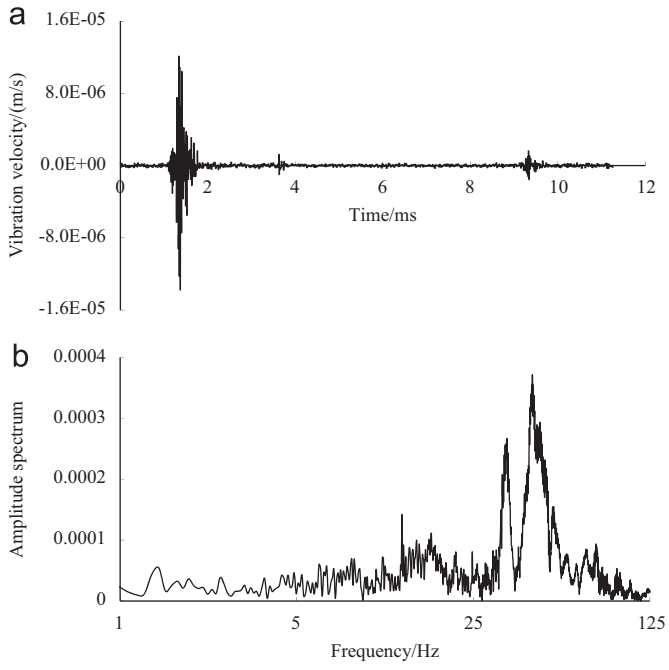

Fig. 6. Curves of vibration velocity-time and amplitude spectrum-frequency (1:47:47-10#). (a) Vibration velocity-time and (b) Amplitude spectrum-frequency.

(Measured results of gas basic parameters are shown in Table 2), and the average thickness is 2.72 m. Roof lithology is generally medium-fine sandstone, and there exists an average 120 m thick hard igneous rock above #10 coal seam 161–185 m, where, the maximum thickness and the average uniaxial compressive strength are 169.18 m and 140 MPa, respectively. Fig. 2 shows the geological units bore column illustration from the hard igneous rock to the floor strata of #10 coal seam. When II1022, II1021, II1024, and II1023 working faces in II102 mining area are all mined completely by sequence, the igneous roof does not overall break yet, the maximum surface subsidence is only 526 mm, and the high stress concentration is formed in the section pillars left between mined working faces and the II1026 driving working face tailentry which vertical average elevation is −650 m. The conducted numerical simulation showed that the igneous rock would not remain stable with a substantial subsidence and the thickness of fracture zone would exceed more than half of the thickness of igneous rock if II1026 working face was mined. Because of the abnormal stress concentration, #10 coal seam will possibly convert to the outburst-prone seam in II102 mining area.

2.3. Description of the coal and gas outburst process

On April 25, 2009, a coal and gas outburst hazard suddenly occurred in II1026 working face tailentry at 1:48 AM. When

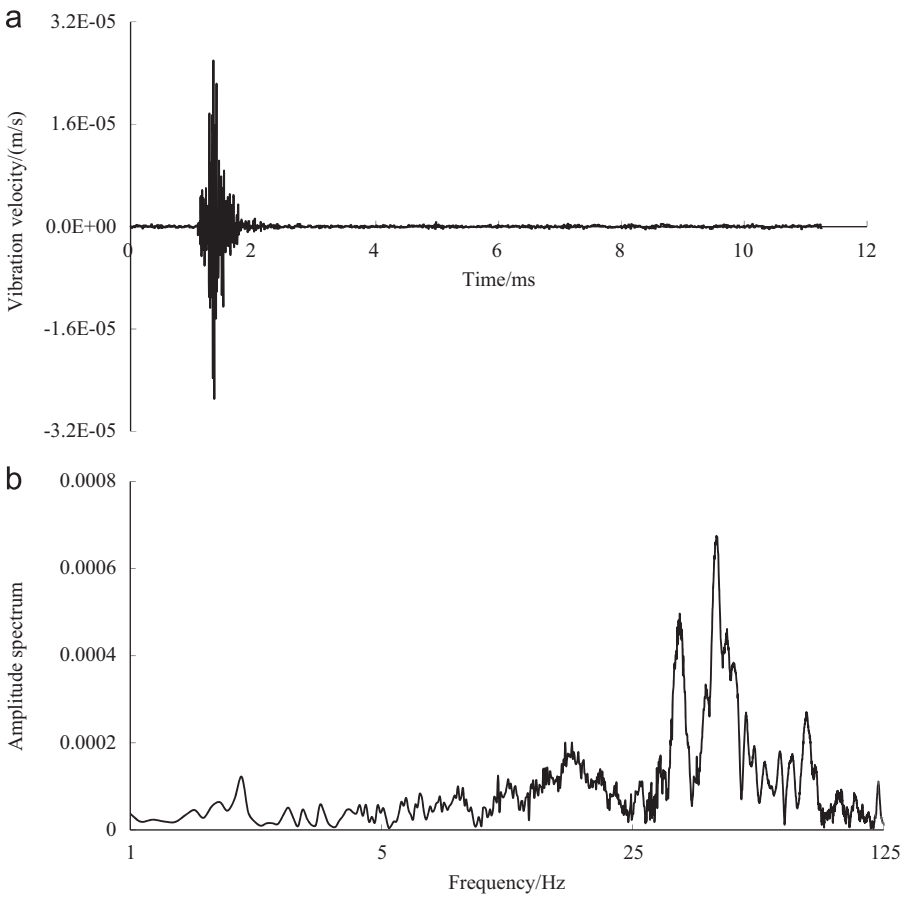

Fig. 7. Curves of vibration velocity-time and amplitude spectrum-frequency (1:48:07-10#). (a) Vibration velocity-time. (b) Amplitude spectrum-frequency.

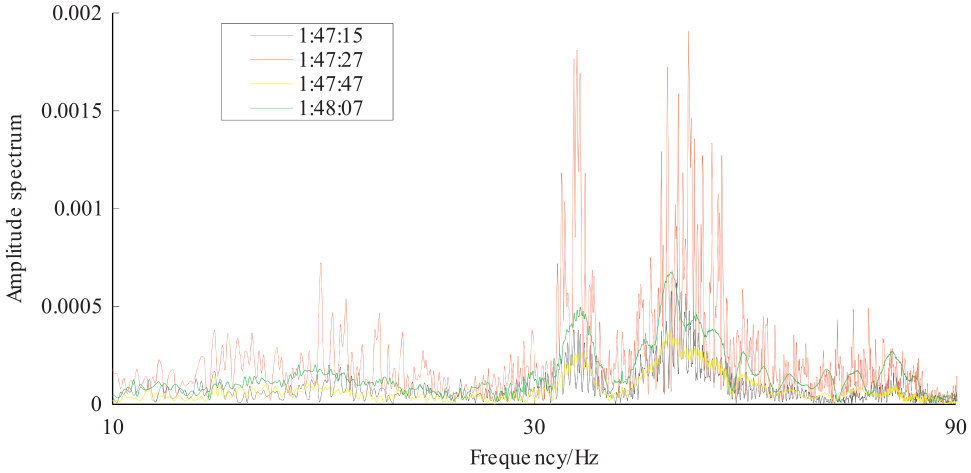

Fig. 8. Comparison of the amplitude spectrum curves of 4 stages of outburst process.

driving distance of tailentry was about 540 m, the head-on coal fracture and the right wall displacement was found, and the immediate roof fracture was sounded like dull thunder, meanwhile began to sink, the outburst happened subsequently. Accumulation length of coal was 74.7 m, the amount of outburst coal was 656 t, and the escaping gas was 13 210 m^3.

2.4. MS monitoring results and analysis

2.4.1. MS monitoring events of outburst

By MS monitoring and analysis, it was found that a shock event appeared in the gob of II1024 working face at 1:47:15 before the outburst and eight shock events occurred near the head-on of II1026 working face tailentry after six seconds. Three signals marked clearly and easily before outburst were recorded on 1:47:15, 1:47:27, and 1:47:47, respectively. By the comparative analysis between the actual position and time of outburst reported by the injured workers and MS system recorded location and time, the outburst occurrence time was determined at 1:48:07. Table 3 showed the total of nine MS events recorded and marked clearly.

Due to the continuous flexural deformation of igneous rock caused by the large mined-out area of II1022, II1021, II1024, and II1023 working faces, the higher stress concentration and limit

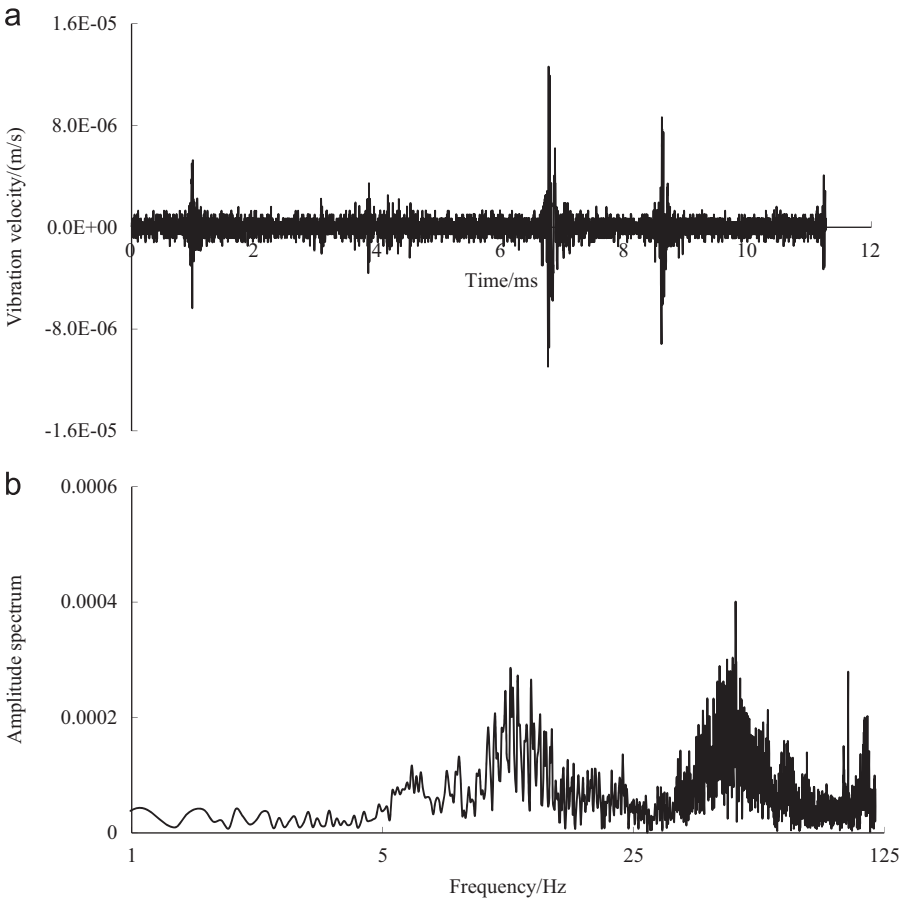

Fig. 9. Curves of vibration velocity-time and amplitude spectrum-frequency (1:47:15-15#). (a) Vibration velocity-time. (b) Amplitude spectrum-frequency.

balance state of coal material of II1026 working face tailentry was formed. Litwiniszyn [23] found that the shock wave might cause the mutation of coal and rock stress, speed, and density, while destroying the coal and rock medium contained gas, and even cause gas phase transition accumulated. Brady et al. [24] revealed that tension force source produced by shock wave of rock catastrophic failure might stimulate the expansion of micro-cracks by the experiments of the electrodynamics of rock fracture. If there are gas and other flow medium in rock, outburst will be induced. Therefore, based on the above research results, once external shock wave disturbance happened, and the outburst disaster may be inevitable.

2.4.2. Wavelet packet coefficient method for processing MS signal

For most shock signals, the low-frequency component is usually the most important part, which can manifest the main features of the signals, while the high-frequency component generally is associated with noise and disturbances, and if the high-frequency part of the signal is removed carefully, the signal key characteristics can still be retained [25]. So, for MS signals recorded by #10 sensor far away from outburst source, due to containing noise and disturbances in the process of propagation, the local high-frequency component can be removed, and the approximate low-frequency component referred should be analyzed in detail.

Wavelet packet coefficient method is used to analyze the high-frequency signal in detail. Wavelet packet is a family of functions, which can construct the L2 (R) orthonormal basis library. For non-stationary signals such as earthquakes and mining shocks, the high-frequency part contains a lot of useful information. Therefore, the wavelet packet is a better analysis of the high-frequency part of signals compared to multi-resolution wavelet. Conventional Fourier transform also can obtain the predominant frequency-spectrum distribution of the mining shock. However, the identification process of signal using the wavelet packet transform is systematic and strong operational [26]. In this paper, the wavelet packet coefficients method was used for noise removal and analysis. At first, a threshold was chosen for processing, the graphical tool of wavelet packet automatically provided an initial threshold, and the default value was 1819659e−06. In most cases, the default threshold is reasonable. Fig. 3 shows the example of waveform data recorded by #10 sensor before and after the noise removal.

For #10 MS sensor, comparative analysis on the waveforms before and after the noise removal showed that the amplitude and waveform distribution did not changed remarkably and only high-frequency noise part has been smoothed. So, it is known that the default threshold is reasonable for processing the noise signals of sensor far away from outburst source.

2.4.3. Analysis on the frequency spectrum characteristic of the outburst signals

Figs. 4–7 show vibration velocity-time and amplitude spectrum-frequency curves of MS signals recorded by #10 sensor far away from source before and during outburst. All original signals was processed and analyzed by the wavelet packet coefficients

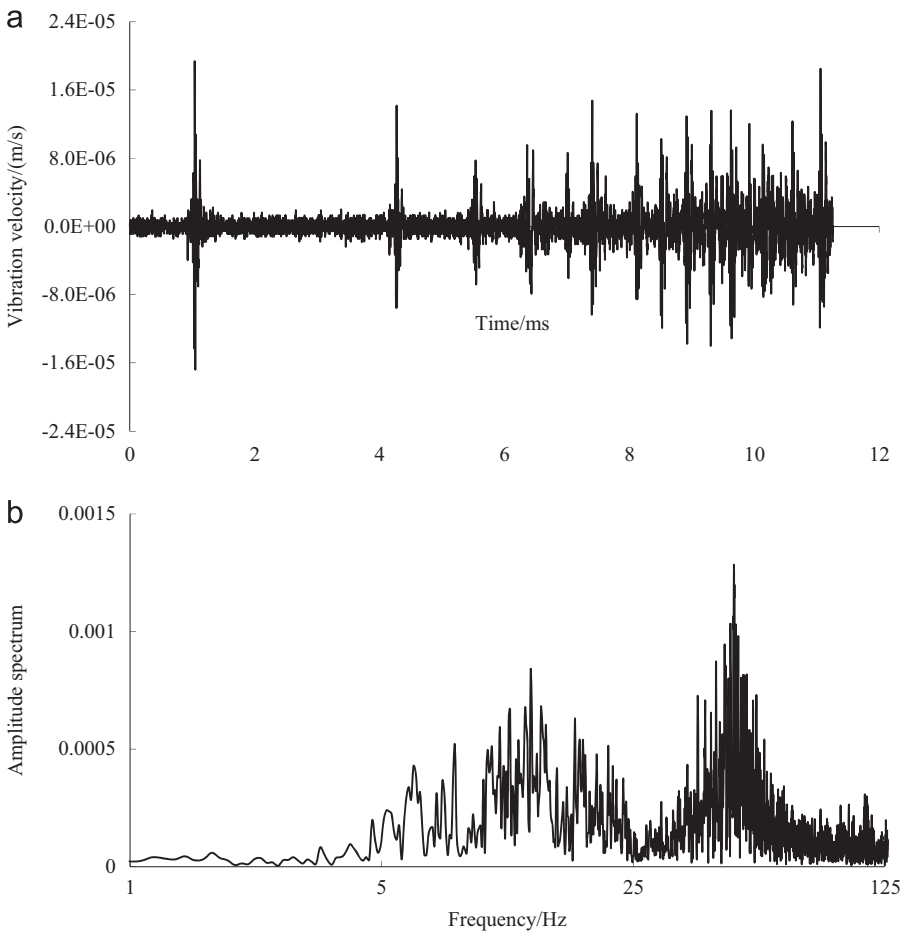

Fig. 10. Curves of vibration velocity-time and amplitude spectrum-frequency (1:47:27-15#). (a) Vibration velocity-time. (b) Amplitude spectrum-frequency.

method. In Figs. 4–7(b), the horizontal logarithmic coordinate (logarithmic scale=5) was used.

From the above figures, it is known that MS waveforms before and during outburst gradually evolved from "continuous multi-peak type" into "single-peak type", and the predominant frequency distribution was 10–90 Hz. According to Figs. 6 and 7(b), the low-frequency (0–5 Hz) component slightly added, which revealed the MS low-frequency precursory effect of outburst process. According to shock wave propagation and attenuation rules [27,28], the precursory effect is less obvious.

Fig. 8 shows the amplitude spectrum curves of 4 stages of the outburst process in the main frequency band of 10–90 Hz. The horizontal logarithmic coordinate (logarithmic scale=3) was used.

From the above figures, it can be known that amplitude spectrum value of MS signal recorded at 1:47:27 was more than four times as much as it is of others in 30–60 Hz high-frequency band, which indicated that micro-fissures had been formed and started to converge in surrounding coal and rock materials of II1026 head-on at 1:47:27. But, after that, the amplitude spectrum value recorded at 1:47:47 sharply reduced because of energy dissipation for connection and convergence of micro-fissures, it might be believed that shock event *d* triggered and accelerated the outburst process.

Because #15 sensor is nearest to the outburst source, it can clearly record the actual outburst signals contained a great deal of high-frequency useful information, and the signals should not easily be filtered and smoothed using wavelet removal which would induce to miss high frequency data as well as low frequency data. Figs. 9–12 show the vibration velocity-time and amplitude spectrum-frequency curves recorded by the #15 sensor closest outburst source before and during outburst. In Figs. 9 and 10(b), the horizontal logarithmic coordinate (logarithmic scale=5) was adopted, and in Figs. 11 and 12(b), the horizontal logarithmic coordinate (logarithmic scale=3) was adopted.

Because #15 sensor is closest to source, it can better reveal MS effect of the whole coal and gas outburst process. Before outburst, the waveforms of MS signals gradually evolved from "continuous multi-peak type" into "single-peak type". At 1:47:15 and 1:47:27, the amplitude spectrum-frequency characteristic curves obviously showed two main frequency distributions of 10–25 Hz and 30–80 Hz bands, respectively. At 1:47:47, as the outburst precursor signal, the 0–10 Hz low-frequency component increased obviously due to macro-fracture formation in coal and rock of II1026 head-on. Another, a significant increase of 90–240 Hz high-frequency component can be observed simultaneously because of a large amount of micro-fissures formation. However, the high-frequency component cannot be effectively recorded by #10 sensor attributed to rapid attenuation of signal. When outburst was induced, the vibration velocity was up to the maximum value, the MS waveform showed the single-peak type and the predominant low-frequency component of 0–10 Hz increased remarkably, which nearly dominated most of the signal energy. Simultaneously, the 90–240 Hz high-frequency component also be recorded which suggested that outburst would produce large amount of micro-fissures.

Fig. 13 shows the total energy bar chart of MS signals recorded and positioned daily in II1026 working face before the coal and gas outburst from March, 25 2009 to April, 24 2009.

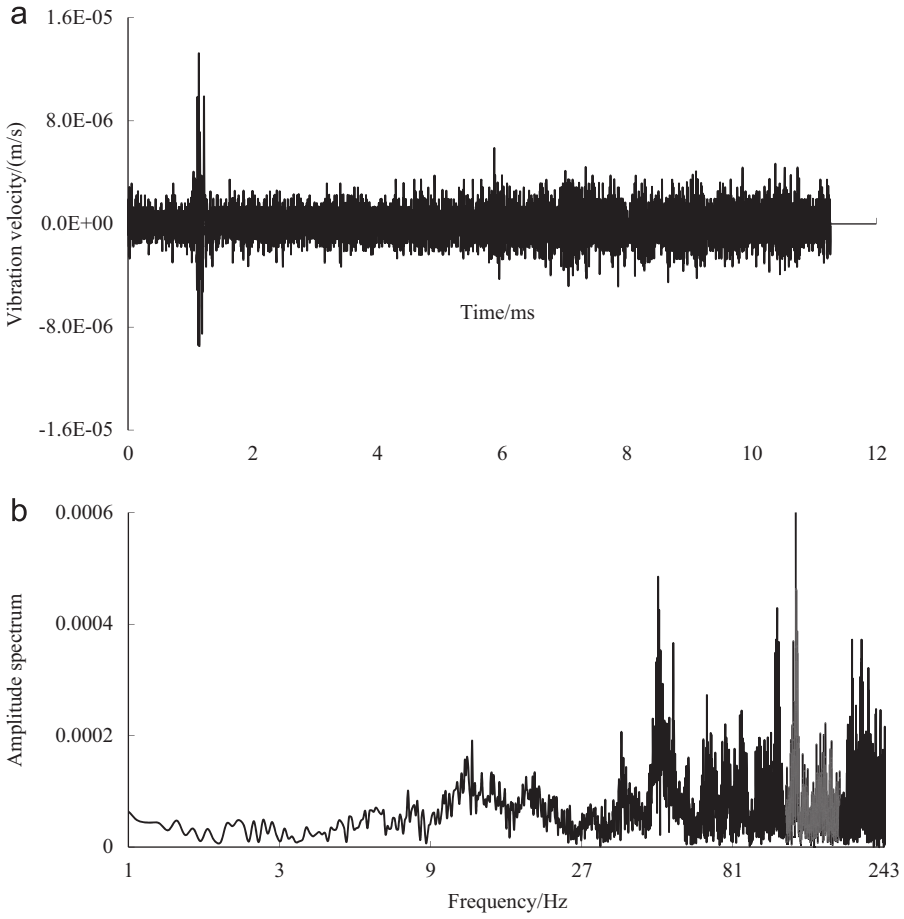

Fig. 11. Curves of vibration velocity-time and amplitude spectrum-frequency (1:47:47-15#). (a) Vibration velocity-time. (b) Amplitude spectrum-frequency.

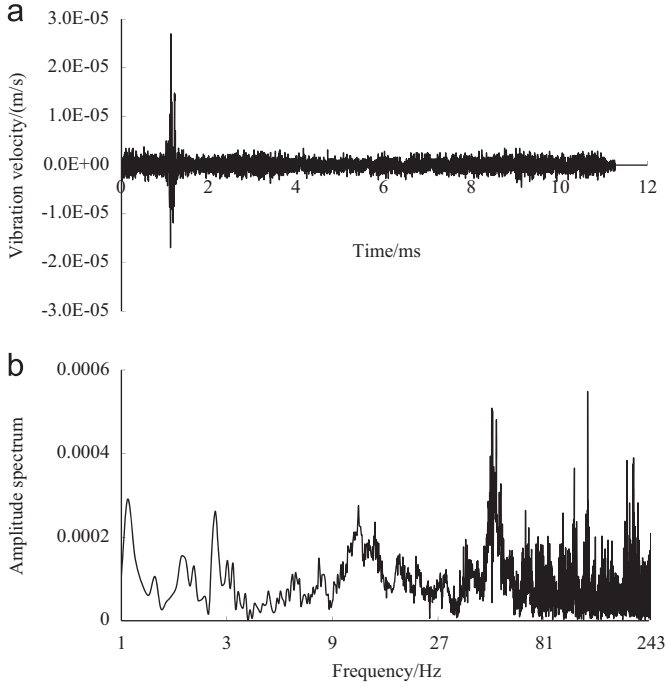

Fig. 12. Curves of vibration velocity-time and amplitude spectrum-frequency (1:48:07-15#). (a) Vibration velocity-time. (b) Amplitude spectrum-frequency.

On the basis of the spot data, the average driving rate of II1026 working face tailentry from March 25 to April 24 was about 4 m/d. From Fig. 13, it can be known that the MS macro-effect manifested the frequent activity and higher energy from March 25 to April 15 before outburst, while a relative MS quiet period and abnormal lower energy from April 16 to April 24, which indicated the continuous energy accumulation in coal and rock materials of II1026 head-on. Finally, the outburst was triggered because of the external shock wave disturbance and the internal higher stress concentration.

3. Conclusions

(1) The main reasons of the outburst include two factors: dynamic load disturbance and static high stress concentration. That is to say, the first is the external shock wave disturbance occurred at 1:47:27, and another is the internal higher stress concentration of II1026 tailentry induced by flexural deformation of igneous rock.

(2) Based on the monitoring and analysis of #10 and #15 sensors, before outburst, the waveforms of MS signals gradually evolve from “continuous multi-peak type” into “single-peak type”, and the frequency spectrum distribution obviously shows two main bands of 10–25 Hz and 30–80 Hz. As the outburst precursor, the 0–10 Hz low-frequency component adds obviously, and a significant increase of 90–240 Hz high-frequency component can also be observed.

(3) When outburst is induced, the vibration velocity was up to the maximum value, MS waveform shows the single-peak type and the predominant low-frequency component of 0–10 Hz increases remarkably, which nearly dominates most of the signal energy. Simultaneously, the 90–240 Hz

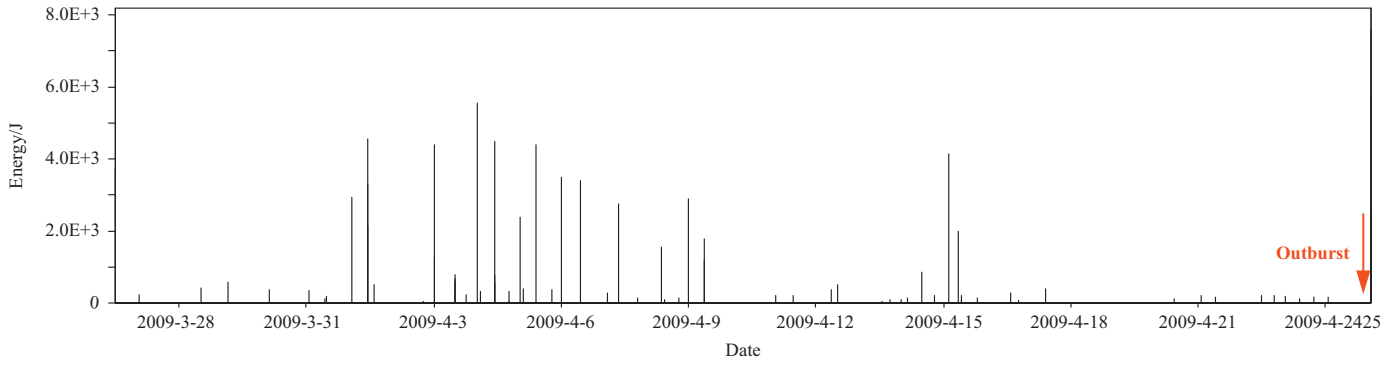

Fig. 13. Bar chart of MS total energy in II1026 working face (2009.3.25-2009.4.24).

high-frequency component also can be recorded which suggests that outburst will produce large amount of micro-fissures.

(4) MS macro-effect of outburst shows as follows: MS frequent activity, low energy release→the relative quiet period, the energy gradual accumulation→induced outburst.

Acknowledgments

First, we are grateful to the editor and unknown referee for suggestions which improved the quality of this note. Second, we gratefully wish to acknowledge the collaborative funding support from the 973 National Basic Research Program (2010CB226805), the Program for New Century Excellent Talents in University (NCET-10-0769), the Foundation for the Author of National Excellent Doctoral Dissertation of PR China (2010044), the "333" Project in Jiangsu Province (BRA2011183), the Project Funded by the Priority Academic Program Development of Jiangsu Higher Education Institutions (SZBF2011-6-B35), Program for Innovative Research Team in University (IRT1084), the Fundamental Research Funds for the Central Universities, "Qinglan Project" in Jiangsu province and Program for Center for Post-doctoral Studies of Huainan Mining Group & Anhui University of Science & Technology. In particular we wish to thank Guo Xiaoqiang, Lu Xinwei, He Hu, and He Jiang for their contributions to this research.

References

[1] Lama RD, Bodziony J. Outbursts of gas, coal and rock in underground coal mines. Scranton, Penn: Int Textbook Co; 1996.
[2] Beamish BB, Crosdale JP. Instantaneous outbursts in underground coal mines: an overview and association with coal type. Int J Coal Geol 1998;35:27–55.
[3] Flores JR. Theoretical study of the reaction of P^+ with methane. J Phys Org Chem 1998;9:419–426.
[4] Lama RD, Bodziony J. Management of outburst in underground coal mines. Int J Coal Geol 1998;35:83–115.
[5] Cao YX, He DD, David CG. Coal and gas outbursts in footwalls of reverse faults. Int J Coal Geol 2001;48:47–63.
[6] Xian XF, Gu M, Li XH, et al. Excitation and occurrence conditions for coal and gas outburst. Rock Soil Mech 2009;30:577–581.
[7] Hu QT, Zhou SN, Zhou XQ. Mechanical mechanism of coal and gas outburst process. J China Coal Soc 2008;33:1368–1372.
[8] Hu QT. Hazard analysis of "5.13" gas and coal blasting in Luling coal mine. Work Prot 2005;3:58–60.
[9] Zhou SN, He XQ. Rheological hypothesis of coal and methane outburst mechanism. J China Univ Min Technol 1990;19:1–8.
[10] He XQ, Zhou GL. Energy dissipation process of coal and gas outburst and non-contact prediction. Coal Sci Technol 1993;21:23–25.
[11] Wang EY, He XQ, Nie BS, et al. Principle of predicting coal and gas outburst using electromagnetic emission. J China Univ Min Technol 2000;29:225–229.
[12] Sa ZY, He XQ, Wang EY. EMR anomaly identification method of coal and gas outburst fatalness. J China Coal Soc 2008;33:1373–1376.
[13] Song WH, Zhang HW. Visualization research on regional prediction of coal and gas outburst based on GIS. J Liaoning Tech Univ 2008;27:337–339.
[14] Tang CA. Research on microseismic precursory rules and monitoring and analyzing technology of mine dynamic disaster. 2006;32–5.
[15] Jiang FX, Wang CW, Yang SH, et al. Microseismic monitoring and measuring technology for pumping pressure, coal and gas outburst and water inrush. Coal Sci Technol 2007;35(26–8):100.
[16] McKavanagh BM, Enever JR. Developing a microseismic outburst warning system. 1978;211–25.
[17] Leighton F. Microseismic activity associated with outbursts in coal mines. 1981;467–77.
[18] Davies AW, Styles P, Jones VK. Developments in outburst prediction by microseismic monitoring from the surface. Min Eng 1987;147:486–498.
[19] Peter S. Implications of harmonic-tremor precursory events for the mechanism of coal and gas outbursts. 1993;415–21.
[20] Stephen DB, Frempong PK, Chinmoy M, et al. Characterization of the permeability and acoustic properties of an outburst-prone sandstone. J Appl Geophys 2006;58:1–12.
[21] María BDA, González CN. Control and prevention of gas outbursts in coal mines, Riosa-Olloniego coalfield, Spain. Int J Coal Geol 2007;69:253–266.
[22] Talebi S, Mottahed P, Corbett GR. Outburst monitoring using microseismic techniques in the Phalen Colliery, Sydney, NovaScotia, Canada, Ottawa. Can Cent Miner Energy Technol 1995.
[23] Litwiniszyn J. Remarks concerning sudden rock-and-gas mass outbursts. Min Sci Technol 1986;3:243–253.
[24] Brady BT, Rowell GA. Laboratory investigation of the electrodynamics of rock fracture. Nature 1986;321:488–492.
[25] Calderoni G, Giovambattista RD, Burrato P, et al. A seismic sequence from Northern Apennines (Italy) provides new insight on the role of fluids in the active tectonics of accretionary wedges. Earth Planet Sci Lett 2009;281:99–109.
[26] Rachel EL, Willsky AS. A wavelet packet approach to transient signal classification. Appl Comput Harmon Anal 1995;2:265–278.
[27] Lu CP, Dou LM, Wu XR, et al. Case study of blast-induced shock wave propagation in coal and rock. Int J Rock Mech Min Sci 2010;47:1046–1054.
[28] Lu CP, Dou LM, Liu B, et al. Microseismic low-frequency precursor effect of bursting failure of coal and rock. J Appl Geophys 2012;79:55–63.